Interactions Between Cationic Conjugated Polyelectrolyte and DNA and a Label-Free Method for DNA Detection Based on Conjugated Polyelectrolyte Complexes

Heng Song, Bin Sun, Ke-Jun Gu, Yan Yang, Yang Zhang, Qun-Dong Shen

Department of Polymer Science and Engineering and Key Laboratory of Mesoscopic Chemistry of MOE, School of Chemistry and Chemical Engineering, Nanjing University, Nanjing 210093, China

Received 20 November 2008; accepted 5 April 2009
DOI 10.1002/app.30566
Published online 18 June 2009 in Wiley InterScience (www.interscience.wiley.com).

ABSTRACT: The electrostatic complexes of single-stranded deoxyribonucleic acid (ssDNA) and a cationic conjugated polyelectrolyte (CPE), poly{9,9-di[3-(1-ethyl-1,1-dimethyl ammonio)propyl]-2,7-fluorenyl-alt-1,4-phenylene dibromide} (PFN), were investigated. Fluorescence emission of PFN solution (10 μmol/L) can be drastically quenched to about one fourth of its original intensity in the presence of a trace amount (2.6 μmol/L) of ssDNA. The effect of oligonucleotide length on the fluorescence quenching behavior was also investigated. In contrast to single-stranded DNA with 20 bases (ssDNA-20), ssDNA with 40 bases (ssDNA-40) induces a relatively higher quenching efficiency and larger red-shift of PFN emission maximum. The binding constant of ssDNA-20 and PFN is estimated to be 1.12×10^{21}. At extremely low concentration (10 nmol/L), PFN can respond to 0.2 nmol/L (or 2×10^{-10} mol/L) of ssDNA-20 by significant enhancement of its emission intensity. The result is contrary to the observation in the relative higher concentration, and its mechanism is postulated. Based on the high binding ability of ssDNA with cationic CPE, a label-free method for ssDNA detection is designed. It uses an electrostatic complex of cationic PFN and an anionic CPE, which exhibits fluorescence resonance energy transfer (FRET) between the two components. Addition of ssDNA improves the FRET extent, indicated by obvious change of fluorescence spectra of the conjugated polyelectrolyte complex. © 2009 Wiley Periodicals, Inc. J Appl Polym Sci 114: 1278–1286, 2009

Key words: conjugated polymers; polyelectrolytes; sensors; fluorescence; water-soluble polymers

INTRODUCTION

Conjugated polyelectrolytes (CPEs) contain π-conjugated backbone with ionic species on the side chains, affording their solubility in water.[1] They constitute a novel class of materials that provide a platform for chemical or biological sensors,[2–5] detection chips,[6] optoelectronic devices,[7–9] etc. CPEs have been applied in the biosensor field, based on their photoluminescence properties on complexation with the target molecules, such as peptides, proteins, deoxyribonucleic acids (DNAs), and ribonucleic acids (RNAs).[10–19] Bazan and coworkers[20–22] have detected DNA by use of fluorescence resonance energy transfer (FRET) from CPEs to fluorophore-labeled peptide nucleic acid (PNA) hybridized with DNA, in which electrostatic attractions between positively charged CPEs and negatively charged phosphate groups in DNA play an important role for their close proximity. Therefore, the interaction between DNAs and CPEs is important for detection. From the previous studies, the interaction of opposite charged analysts influences chain conformation, aggregation, and thereby fluorescence of CPEs,[23–25] which in turn affects the signal output of DNA detection. It occurs to us that the interaction between CPEs and DNAs must be thoroughly understood. Besides, many assays require to use fluorophore-labeled DNAs, which would increase the cost and the complication of the detection process. Hence, a label-free method is required for research in this field. Furthermore, electrostatic interaction between CPEs and single-stranded DNAs attached on solid substrates, such as silicon wafer or glass, is essential to build up DNA detection chips. For practical application, ssDNA may be presented in an extremely diluted solution and various sequence lengths, which would make the detection diversified. These effects must be carefully considered.

In this contribution, we focus on the interaction between ssDNA and a cationic CPE, poly{9,9-di[3-(1-ethyl-1,1-dimethylammonio)propyl]-2,7-fluorenyl-alt-1,4-phenylene dibromide} (PFN) by analyzing fluorescence emission spectra of PFN in the presence of different sequence lengths of ssDNA. A simple

Correspondence to: Q.-D. Shen (qdshen@nju.edu.cn).
Contract grant sponsor: National Natural Science Foundation of China; contract grant number: 20774040.

model was applied to study binding ability of ssDNA with PFN. Fluorescence response of PFN to ssDNA at extremely low concentration was also investigated to find out the ssDNA detection limit by the current system and to indicate the concentration effect on the interaction mechanism. A label-free method for ssDNA detection was also developed by using an electrostatic complex of cationic PFN and an anionic conjugated polyelectrolyte, poly[sodium 9,9-di(3-sulfonatopropyl)-2,7-fluorenyl-alt-2,5-thienyl] (Th-PFS), which exhibits the FRET process between both components. Tight binding of ssDNA to the complex interrupts the FRET process. This label-free method is easy to perform for rapid ssDNA analysis with detection limit of 4 μmol/L and may extend to the analysis of diversified sequence DNAs, based on their different binding abilities with PFN.

EXPERIMENTAL SECTION

Materials

Potassium 2,7-dibromo-9,9-bis(3′-sulfonatopropyl)-fluorene and PFN were synthesized as previously reported.[26,27] The single-stranded oligonucleotides, 5′-ACCACCTACCAAGTTAGTAC-3′ (ssDNA-20) and 5′-CTTGGAGTGTATACTGTCTACATACGTGTT GATCGATTCT-3′ (ssDNA-40) was purchased from Invitrogen Corporation (Shanghai, China). 2-Isopropoxy-4,4,5,5- tetramethyl-1,3,2-dioxaborolane, *n*-butyllithium in 2 mol/L cyclohexane solution and tetrakis(triphenylphosphine) palladium (0) were purchased from Aldrich Chemical Company (Milwaukee, WI) and used as received. Anhydrous tetrahydrofuran (THF) was obtained by distillation over sodium before use. All other chemicals were used without further purification.

2,5-bis(4,4,5,5-tetramethyl-1,3,2-dioxaborolan-2-Yl)thiophene[28]

n-Butyllithium in 2 mol/L cyclohexane solution (8.68 mL, 17.4 mmol) was added dropwise into a solution of 2,5-dibromothiophene (2.29 g, 9.47 mmol) in 50 mL of anhydrous THF kept at −78°C under an atmosphere of dry nitrogen. The mixture was stirred at −78°C for 1 h. Then 2-isopropoxy-4,4,5,5-tetramethyl-1,3,2-dioxaborolane (10 mL, 49 mmol) was injected promptly into the flask. The mixture was stirred at −78°C for 1 h and then allowed to stand overnight at room temperature. The mixture was poured into water and extracted with ethyl acetate. The extract was washed with brine and dried over anhydrous magnesium sulfate. After evaporation of the solvent, the residue was recrystallized from hexane/chloroform to afford 1.78 g of white solid (yield, 56%); ^{1}H-NMR ($CDCl_3$) δ (ppm): 7.68 (s, 2 H), 1.33 (s, 24 H).

Poly[sodium 9,9-di(3-sulfonatopropyl)-2,7-fluorenyl-Alt-2,5-thienyl] (Th-PFS)

Th-PFS was obtained by the Suzuki coupling method[27] from an equivalent molar mixture of potassium 2,7-dibromo-9,9-bis(3′-sulfonatopropyl) fluorene and 2,5-bis(4,4,5,5-tetramethyl-1,3,2-dioxaborolan-2-yl) thiophene by use of tetrakis (triphenylphosphine) palladium (0) as catalyst. The as-prepared conjugated polyelectrolyte was purified by dialysis in distilled water using a membrane with cutoff molecular weight of 8000 to 10,000 g/mol for 3 days.

Fluorescence titration experiment

A stock solution containing 0.2 μmol/L ssDNA in 0.1 mol/L phosphate-buffer solution (PBS, pH 7.4) was prepared and incubated for 30 min. An appropriate amount of the ssDNA solution was mixed with 3 mL of the conjugated polyelectrolyte solution to give the desired concentration of single-stranded oligonucleotide. After 5 min of incubation, the emission spectra were recorded with RF-5310PC (Shimadzu, Japan) luminescence spectrometer. The spectra were recorded with excitation at 370 nm.

Characterization

^{1}H-NMR spectra were collected on a Bruker DPX300 spectrometer (Bruker, Switzerland).

RESULTS AND DISCUSSION

Fluorescence quenching of cationic conjugated electrolyte by ssDNA

PFN (Scheme 1) is cationic water-soluble conjugated polyelectrolyte and can be used as light-harvesting molecules with high fluorescence quantum yield (82% measured at room temperature by use of 1×10^{-5} mol/L quinine sulphate in 0.1 mol/L sulfuric acid as the standard), whereas single-stranded oligonucleotide (ssDNA) carries highly electronegative charges on phosphate groups. They can form complexes through electrostatic interaction. Addition of ssDNA with 20 bases (ssDNA-20) to PFN (10 μmol/L in repeat unit, the following concentration is calculated in the same way) in the PBS solution results in the fluorescence quenching of the latter [Fig. 1(a)]. As the ssDNA-20 concentration increases from 0 to 2.6 μmol/L, the photoluminescence (PL) intensity of the cationic conjugated polyelectrolyte decreases to only a quarter of the PL intensity in the absence of ssDNA-20. It is also noteworthy that ssDNA-20 leads to amplified fluorescence quenching concomitant with slight red-shift of PFN emission maximum from 415 to 418 nm [Fig. 1(b)].

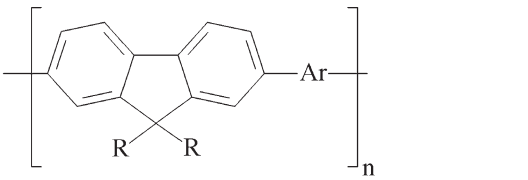

PFN R = $-(CH_2)_3N^+(CH_3)_2(C_2H_5)Br^-$ Ar =

Th-PFS R= $-(CH_2)_3SO_3^-\,Na^+$ Ar =

Scheme 1 Chemical structure of cationic and anionic polyelectrolytes described in the text.

The quenching process can be quantitatively described by the Stern-Volmer equation:

$$\frac{PL_0}{PL} = 1 + K_{SV}[Q]$$

where the PL_0 and PL are the intensity of fluorescence in the absence and in the presence of ssDNA, respectively; whereas [Q] is concentration of the quencher (ssDNA). K_{SV} is the Stern-Volmer constant, which provides a quantitative measure of quenching efficiency. The Stern-Volmer plot of PFN quenched by ssDNA-20 is shown in the inset of Figure 1(a). At ssDNA-20 concentration ranging from 0 to 1.2 μmol/L, a linear plot with $K_{SV} = 6.4 \times 10^5$ $mol^{-1}L$ is obtained. The quenching efficiency is pronounced if one considers a fluorescence quenching system of small molecule-weight stilbene and methylviologen whose K_{SV} is as low as 15.[3] The extremely large quenching efficiency arises at least from two effects. First, in view of their negative charges, the ssDNA molecules are expected to readily bind positively charged conjugated polymer chains by a combination of coulombic and entropic interactions, which brings about an effect of local concentration enhancement of PFN. This indicates the accessibility and thereby high sensibility of PFN to ssDNA. Second, the conjugated polyelectrolyte is characterized by a "molecular wire" effect. It regards an isolated conjugated polymer chain as a highly efficient transport medium of the electronic excited states (excitons). As a result, binding events at a site might be sensed by a whole chain, leading to amplifying the fluorescent system.[29]

Effect of ssDNA length on its interaction with cationic CPE

It has been demonstrated that single-stranded DNA with sequence length of 20 is sufficient for tight binding of PFN. Thus the question arises of whether ssDNA with a larger number of bases might induce a different secondary structure of their electrostatic complexes and thereby change the fluorescence behaviors of the conjugated polyelectrolytes in a different way. A binding study was conducted on an oligonucleotide with 40 bases (ssDNA-40). As shown in the Figure 2(a), the fluorescence intensity of PFN (10 μmol/L) in the presence of 2.6 μmol/L ssDNA-40 decreases to less than a fifth of its original intensity in the absence of ssDNA-40. Meanwhile, the normalized spectrum is obviously red-shifted from 415 to 449 nm [Fig. 2(b)]. K_{SV} value is 9.2×10^5 $mol^{-1}L$ at ssDNA-40 concentration ranging from 0 to 1.2 μmol/L [inset of Fig. 2(a)]. Higher quenching efficiency and larger red-shifted emission maximum of ssDNA-40 than those of ssDNA-20 indicate high-

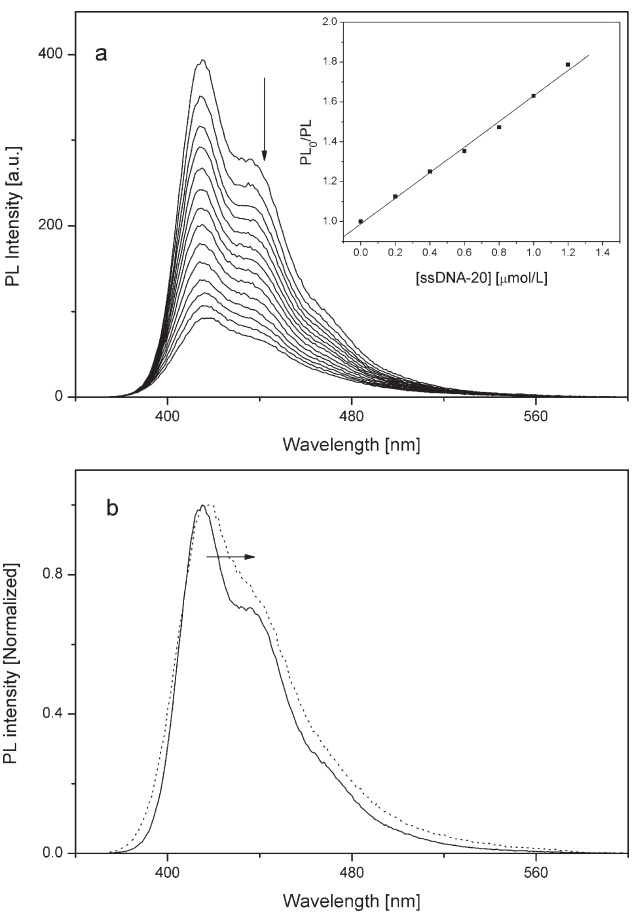

Figure 1 (a) Fluorescence emission spectra of PFN (10 μmol/L) in PBS with successive additions of ssDNA-20 (from 0 to 2.6 μmol/L). Each curve corresponds to an ssDNA-20 concentration increment of 0.2 μmol/L. The inset shows Stern-Volmer quenching plot. (b) The normalized fluorescence emission spectra of PFN in the absence (solid line) and presence (dotted line) of 2.6 μmol/L ssDNA-20. Arrows indicate direction of change in emission with addition of ssDNA-20. The excitation wavelength is 370 nm.

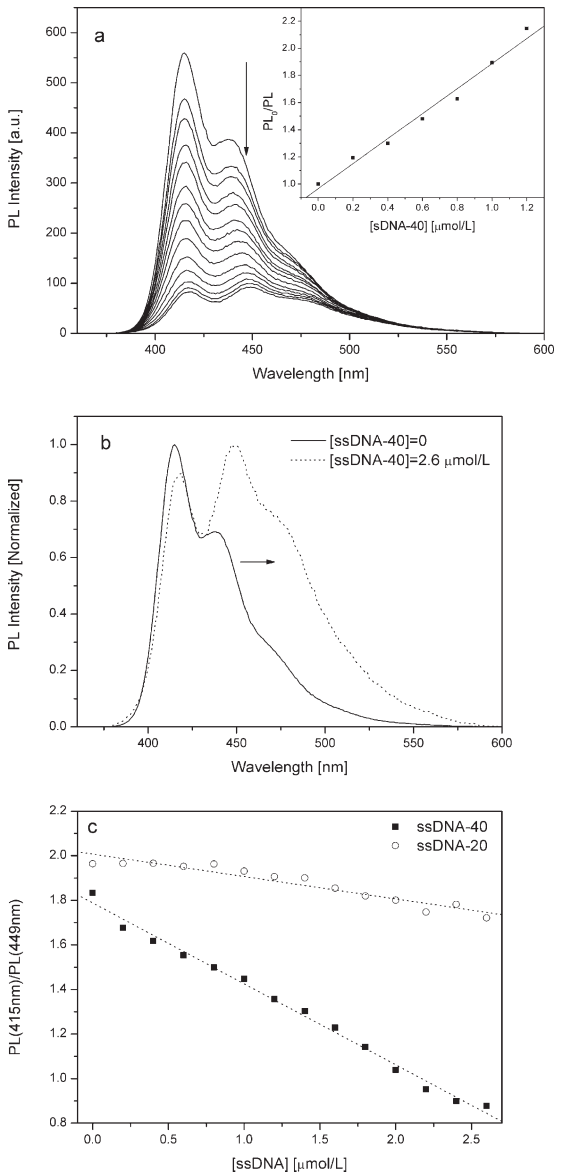

Figure 2 (a) Fluorescence emission spectra of PFN (10 μmol/L) in PBS with successive additions of ssDNA-40. The inset shows Stern-Volmer quenching plot. (b) The normalized fluorescence emission spectrum of PFN in the absence (solid line) and presence (dotted line) of 2.6 μmol/L ssDNA-40. (c) The fluorescence intensity ratio at 415 and 449 nm. The excitation is at 370 nm.

affinitive binding of PFN to single-stranded DNA with more bases.

The fluorescence spectra of PFN can be deconvoluted into several peaks that might arise from the presence of the distribution of conjugation lengths caused by different degree of conformation disorder in the conjugated polymer chains. The peak at 415 nm is more sensitive to ssDNA-40 than that at longer wavelength. The degree of red-shift can be given by the fluorescence intensity ratio at 415 and 449 nm [Fig. 2(c)], from which one can easily distinguish ssDNA-20 from ssDNA-40.

Binding constant of cationic CPE and ssDNA

According to the results shown above, the length of ssDNA has particular effect on emission spectra of PFN. Therefore, a simple electrostatic binding model is constituted to evaluate the binding ability of two kinds of ssDNA molecules to PFN. If one supposes that one single chain of ssDNA would bind several cationic conjugated polyelectrolyte chains, the formation of PFN/ssDNA complexes could be expressed as following equation:

$$\text{ssDNA} + n\text{PFN} \rightleftharpoons \text{ssDNA} - \text{PFN}_n$$

where n represents the number of conjugated polymer chains binding to a single ssDNA molecule. The electrostatic complex is simplified to ssDNA – PFN_n.

The binding constant K_b is written as:

$$K_b = \frac{[\text{ssDNA} - \text{PFN}_n]}{[\text{ssDNA}] \times [\text{PFN}]^n} = \frac{([\text{PFN}]_0 - [\text{PFN}])/n}{\{[\text{ssDNA}]_0 - ([\text{PFN}]_0 - [\text{PFN}])/n\} \times [\text{PFN}]^n} \quad (1)$$

where the substance concentration free from complexation is given as [PFN] and [ssDNA]; $[\text{PFN}]_0$ (10 μmol/L) or $[\text{ssDNA}]_0$ is the initial concentration.

One might expect that the fluorescence of the ssDNA and PFN mixture mainly comes from highly emissive PFN free from complexation and the weakly emissive electrostatic complexes, i.e., ssDNA – PFN_n. It should be assumed that, in the presence of excessive ssDNA, the emission intensity of PFN becomes constant with a value of PL_c. Next, emission intensity is postulated to be directly proportional to the sample concentration, thereby the overall emission intensity (PL) is given by:

$$\text{PL} = \frac{[\text{PFN}] \times \text{PL}_0 + ([\text{PFN}]_0 - [\text{PFN}]) \times \text{PL}_c}{[\text{PFN}]_0} \quad (2)$$

Using eqs. (1) and (2), the relationship between [ssDNA] and the PL intensity is obtained.

The best fit of our experimental data [solid line in Fig. 3(a)] yields binding constant (1.12×10^{21}) of ssDNA-20 with PFN. For comparison, the binding constant for Histone H4 peptide, DnaB protein, and cetyltrimethylammonium bromide (CTAB) to single-stranded DNA is found to be 1×10^{10}, 6×10^6, and 8.7×10^4, respectively.[30–32] This may be attributed to the high charge density of PFN and ssDNA, leading to more interaction sites for the binding process. The extremely large binding constant of the ssDNA results in PFN quenching process that is static in nature, whereas dynamic quenching due to diffusion of the ssDNA free from complexation to an excited state of conjugated polyelectrolyte is insignificant. In

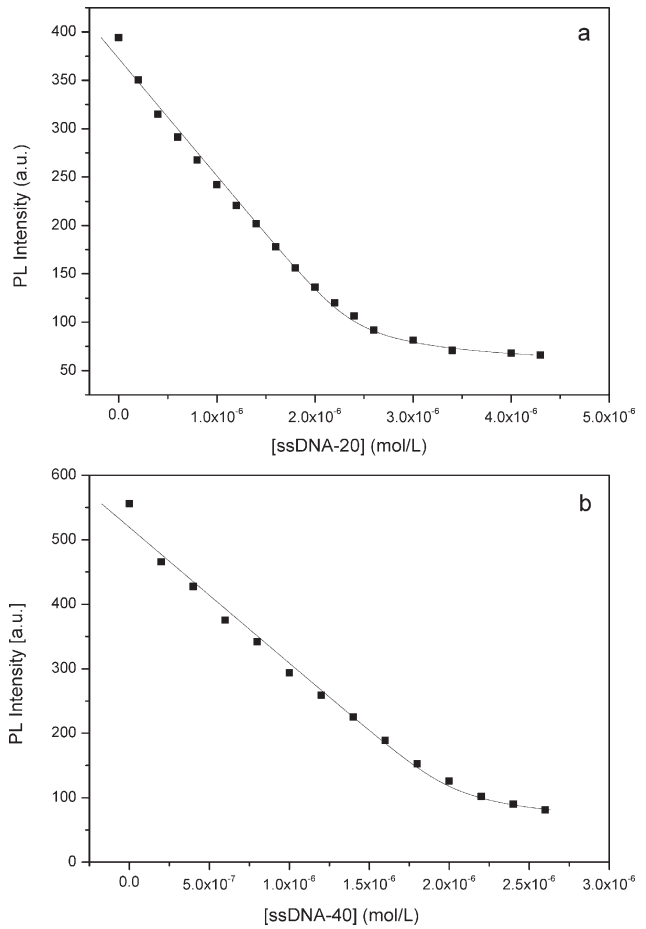

Figure 3 Evolution of fluorescence intensity of PFN at emission maximum with (a) ssDNA-20 and (b) ssDNA-40. Solid curves are best fits by eqs. (1) and (2).

other words, once the electrostatic complexes are generated, the excited state of PFN is quenched immediately and quantitatively.

A simple cationic and anionic polyelectrolyte interaction can be described by a 1 : 1 stoichiometry. However, the number of PFN binding to ssDNA-20 is best fitted to be 3.5. It might be ascribed to multivalence (multiple binding sites) of the target DNA, which leads to self-aggregations of the conjugated polyelectrolyte chains. One can infer from its chemical structure that the driving force for the aggregation of PFN is the hydrophobic interaction, i.e., π-stacking of aromatic rings. Highly efficient fluorescence turn-off by the ssDNA thereby might come from the formation of weakly emissive interchain species of the conjugated polymers.[33]

On the basis of fluorescence titration curves, ssDNA-40 binds considerably more tightly to PFN than ssDNA-20 with binding constant of 5.23×10^{24} [Fig. 3(b)]. In contrast, the number of PFN binding with ssDNA-40 only slightly changes to 4.1. It indicates that single-stranded DNA with longer sequence length induces nearly the same aggregation degree of PFN. It is easily seen that supramolecular structure of the conjugated polyelectrolyte and oppositely ssDNA molecules is crucial to their fluorescence behaviors, but more detailed structure is still unknown.

Fluorescence behavior of ssDNA/PFN at extremely low concentration

Since PFN is highly emissive, one can detect its fluorescence spectra at concentration as low as 10 nmol/L in PBS. This provides an opportunity to analyze trace amounts of ssDNA. As shown in Figure 4, when merely 0.2 nmol/L of ssDNA-20 is added, PFN emission intensity increases remarkably. It means that PFN is a valuable candidate for lowering the detection limit of ssDNA. The high sensitivity of PFN can be ascribed to its high fluorescence quantum efficiency, molecular wire effect, as well as the high stability of the PFN/ssDNA complexes. The emission maximum of PFN is red-shifted from 420 to 428 nm (inset of Fig. 4). In the presence of ssDNA-20, the fluorescence behavior, i.e., enhanced emission and obvious red-shift, of PFN at a concentration of 10 nmol/L is different from that of PFN at a concentration of 10 μmol/L. In the latter case, fluorescence quenching is accompanied by slight red-shift. It indicates a different way of interaction between the conjugated polyelectrolyte and ssDNA at extremely low concentration, which will be discussed later.

It is anticipated that there is a turning point of fluorescence response of PFN to ssDNA when the conjugated polyelectrolyte changes its concentration from 10 nmol/L to 10 μmol/L. The fluorescence response of PFN with a concentration of 0.1 μmol/L to ssDNA was recorded. As can be seen in Figure 5,

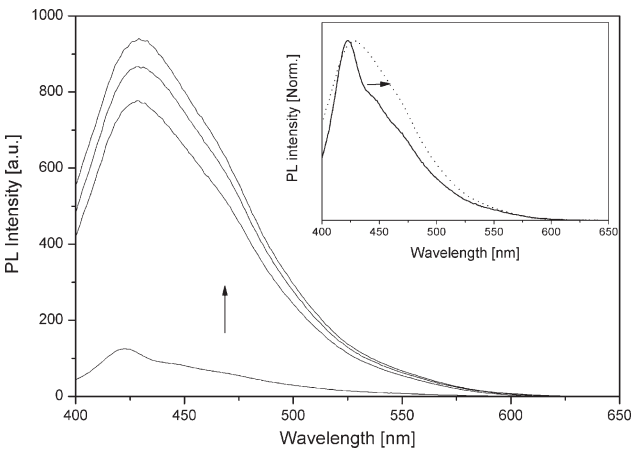

Figure 4 Response of emission spectra of PFN (10 nmol/L) to ssDNA-20 with concentration increment of 0.2 nmol/L. Inset: Normalized emission spectra of PFN in the absence (solid line) and in the presence of ssDNA (0.2 nmol/L, dotted line). Arrows indicate direction of change in emission with addition of ssDNA-20. The excitation is at 370 nm.

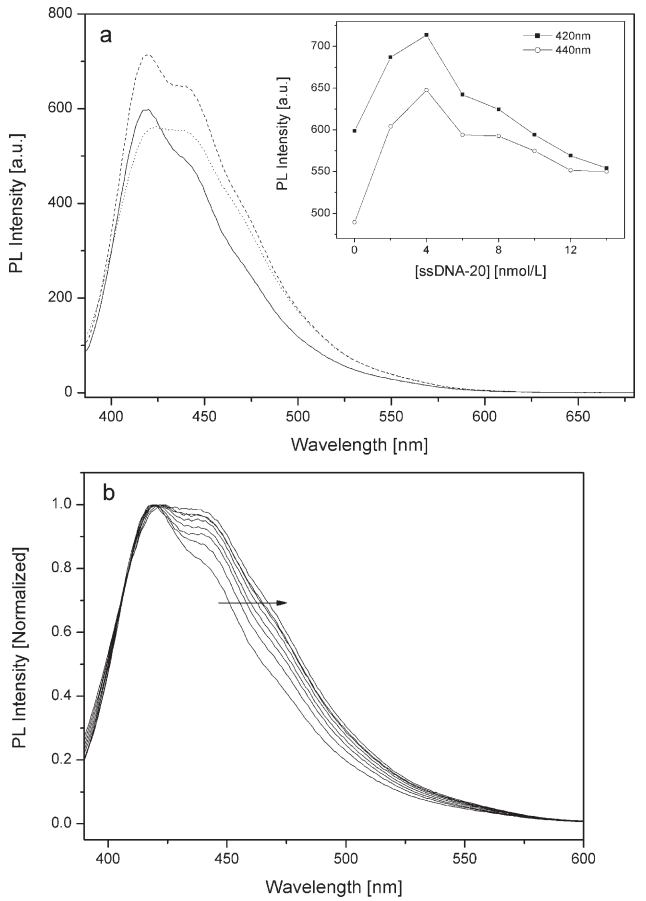

Figure 5 (a) Change of PFN (0.1 μmol/L, solid line) emission spectra in the presence of 4 nmol/L (dashed line) and 14 nmol/L (dotted line) of ssDNA-20. Inset: Dependence of PFN emission intensity on ssDNA-20 concentration. (b) Normalized spectra of PFN in the presence of ssDNA with concentration increased by 2 nmol/L each (from left to right). The excitation is at 370 nm.

with the introduction of ssDNA-20 at a concentration less than 4 nmol/L, there is first a fast increase of emission intensity of the conjugated polyelectrolyte. The fluorescence monitored at 420 and 440 nm then undergoes decrease by continuous addition of ssDNA [inset of Fig. 5(a)]. It appears that the response of PFN fluorescence spectra to ssDNA is diversified at a certain polymer concentration, for example, 0.1 μmol/L.

Mechanism of interaction between PFN and ssDNA

It is noteworthy to elucidate the fundamental processes correlated with the amplified fluorescence quenching or enhancement of PFN at different concentrations. Besides strong electrostatic forces between oppositely charged PFN and ssDNA, two factors associated with the structure change of the conjugated polyelectrolyte during complexation should be taken into account.

First, the chain conformation (planar or nonplanar) or effective conjugation length of the conjugated polymers can be changed by interaction with the analytic molecules. Due to the backbone twisting caused by the steric effect of side groups, conjugated polymers might take different chain conformations and adopt a molecular geometry of random coil. It has been proved that cationic surfactant can induce conformational transition of poly {[2-methoxy-5-(3-sulfonatopropoxy)-1,4-phenylene]-1,2-ethenediyl} (MPS-PPV), an anionic conjugated polyelectrolyte, from random coil to more extended chain, resulting in red-shift of emission spectra and an increase of fluorescence quantum yield.[23]

Second, isolated single chains of PFN (an amphiphilic polyelectrolyte) have a tendency to self-assemble in water through hydrophobic interaction of their aromatic rings. The proposed structure of the aggregates is a tightly packed hydrophobic interior surrounded by a hydrophilic outer surface with cationic ammonium groups extended into water. During strong electrostatic binding to oppositely charged analytes (ssDNA), the hydrophobic nature of its conjugated backbone is of particular importance in the formation of association complexes in aqueous media. The aggregation of PFN can be perceived through monitoring its photoluminescence spectra at different solvent compositions. As shown in the Figure 6, addition of an organic solvent (methanol, MeOH) into PFN aqueous solution enhances its PL intensity, and a slight blue-shift of emission maximum is observed at the same time. Due to strong interactions between hydrophobic conjugated backbones and methanol molecules, increased solubility tends to break up PFN aggregation. Therefore, highly emissive intrachain excitons replace weakly emissive interchain excitons, which results in an increase in quantum yield and a slight blue-shift of emission peak.

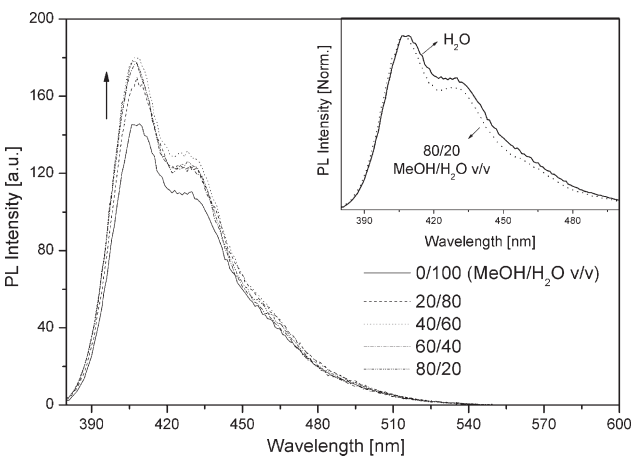

Figure 6 Solvent (methanol) effect on fluorescence emission of PFN (1 μmol/L).

The attractive interaction between cationic PFN and oppositely charged ssDNA molecules gradually neutralizes their charges. The aggregates of the conjugated polyelectrolyte become more hydrophobic with depletion of water molecules, which induces more weakly emissive interchain excitons. The fluorescence quenching of PFN (10 μmol/L) by ssDNA-20 accompanied by small spectral red-shift (Figs. 1 and 2) could be ascribed to aggregation induced by electrostatic complexation and is consistent with the results of the electrostatic binding model, in which every ssDNA molecule binds about four conjugated polymer chains.

Interaction between water-soluble PFN and the oppositely charged ssDNA at an extremely low concentration is more complicated. Fluorescence enhancement of 10 nmol/L PFN (Fig. 4) can be ascribed to either structure change from folded coil to more extended chain or elimination of the chain aggregations. The emission peak is slightly red-shifted with the involvement of ssDNA. Conformational change of the conjugated polyelectrolytes is more likely than dissociation of aggregation, because blue-shift is expected in the later case.

It appears that electrostatic complexation changes both chain conformation and aggregation degree of the conjugated polyelectrolyte, whereas the contribution of these two effects varies with PFN concentration. Complexation-induced aggregation dominates at high concentration, whereas conformational change plays an important role at extremely low concentration of PFN. At moderate concentration, both effects might be observed, as shown in Figure 5.

PFN/Th-PFS electrostatic complex for ssDNA detection

Based on the above discussion, complexation of PFN and ssDNA could result in spectral shift and modification of fluorescence quantum yield, which is a useful indication for ultra-sensitive detection of ssDNA. One remaining problem is that the sensory signal transduction of ssDNA with the intrinsic fluorescence of PFN is dependent on concentration of the conjugated polyelectrolyte. One should also recognize that monitoring emission intensity might be blurred by background fluorescence in a real biological environment. In contrast, shape change of fluorescence spectra in the presence of analytes is more reliable. Therefore, a label-free method for DNA detection has been designed, using electrostatic complexes of cationic and anionic CPEs, which exhibits fluorescence resonance energy transfer (FRET) between the two components. The anionic CPE used here is a polyfluorene derivative alternately incorporating thiophene units (Th-PFS as shown in Scheme 1), whereas PFN is alternating copolymer of fluorene and benzene units. The emission maxima are obviously changed by the type of alternating units. Compared with PFN, Th-PFS has emission maximum red-shifted to 463 nm [Fig. 7(a)]. In aqueous solution, absorptions of these two conjugated polymers arise from π-electron transitions from delocalized occupied molecular orbital to delocalized unoccupied one, and the photoexcited molecules then return to the ground state by emitting visible light. Therefore, different electronic properties of the alternating units are responsible for the red-shift of Th-PFS fluorescence spectrum. The highest occupied molecular orbital (HOMO) level of Th-PFS is increased because of the electron-donor characteristic of the thiophene units. Increase in the HOMO energy reduces the HOMO-LUMO (lowest unoccupied molecular orbital) gap and accordingly reduces the energy of the photon that the conjugated polymer emits.

As shown in Figure 7(a), electrostatic complexation of Th-PFS and PFN results in an obvious change of the fluorescence spectra. The PL intensity of PFN is quenched when mixing with Th-PFS, whereas the emission maximum of the complexes is found at 484 nm. With the introduction of ssDNA to the PFN/Th-PFS solution, it could be seen that the photoluminescence signal at 419 nm decreases and the emission at 484 nm increases [Fig. 7(b)]. Compared with PFN alone, the electrostatic complexes of the cationic and anionic conjugated polyelectrolytes afford spectral shape change rather than emission intensity attenuation, which is more reliable for fluorescence signal output.

As shown in Figure 7(c), there is good fluorescence and absorption spectral overlap between these two conjugated polyelectrolytes. As we know, when the fluorescence spectrum of one fluorophore (the donor) overlaps with the excitation spectrum of another fluorophore (the acceptor), excitation of the donor induces emission of the acceptor at the cost of fluorescence quenching of the former. Such an interesting fluorescence-related phenomenon called FRET is extremely sensitive to the distance between the donor and the acceptor. The complexation of blue-emissive PFN with green-emissive Th-PFS shortens the distance of both components and induces the FRET process. Because the extent of FRET is inversely proportional to the sixth power of the distance, enhancement of Th-PFS emission accompanied by fluorescence quenching of PFN in the presence of ssDNA-20 indicates close proximity of the conjugated polyelectrolytes, which makes energy transfer more efficient. Driving forces for the complexation of ssDNA with PFN/Th-PFS may come from two aspects. First, there are hydrophobic interactions between aromatic units in the conjugated polyelectrolytes and ssDNA bases.[34] Second, the excess

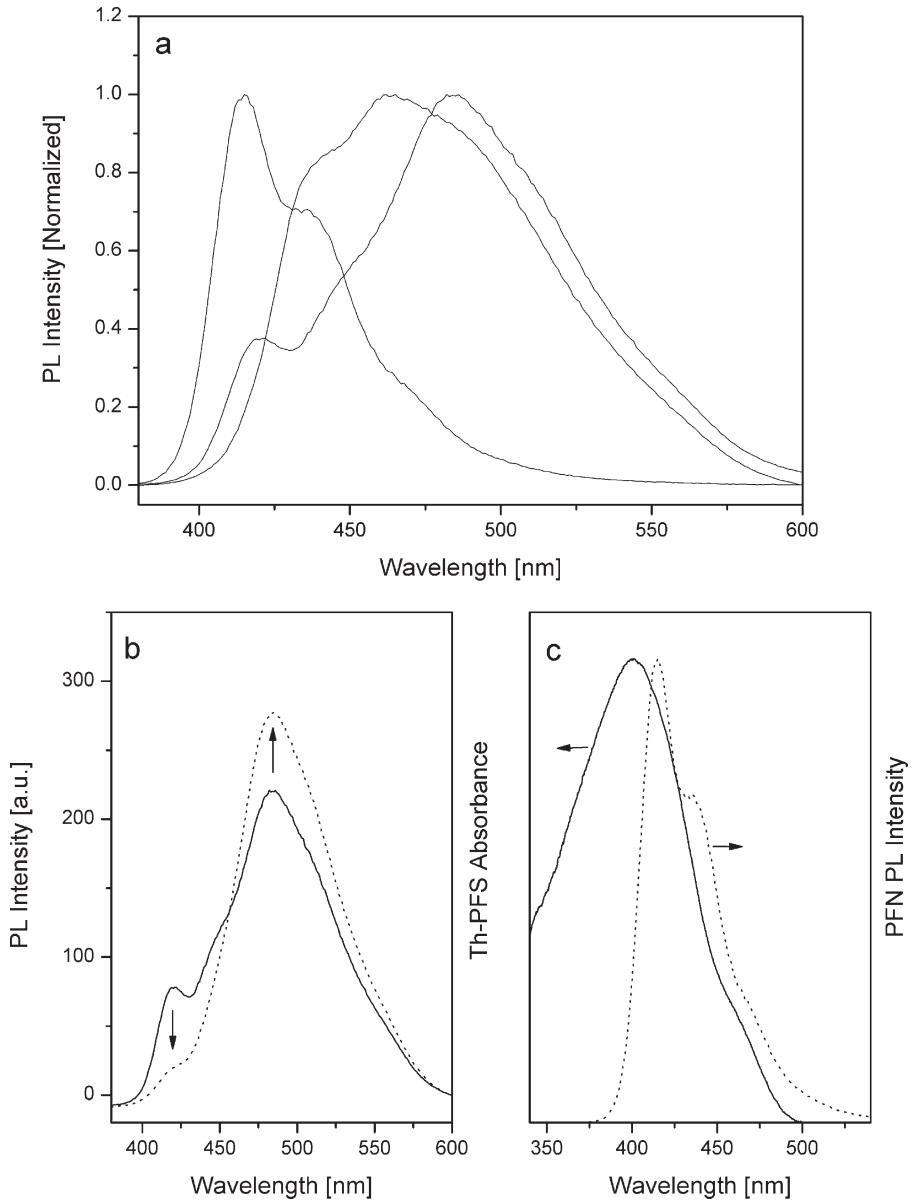

Figure 7 (a) Emission spectra of PFN, Th-PFS, and their complex (1 : 1 mol/mol). Emission maximum moves from left to right. (b) Emission spectra of the electrostatic complex of PFN (5 μmol/L) and Th-PFS (5 μmol/L) in the absence (solid line) and presence of 4 μmol/L ssDNA-20 (dotted line). Arrows indicate direction of change in emission with addition of ssDNA. (c) Fluorescence spectrum of PFN (dotted line) overlaps well with electron absorption spectrum of Th-PFS (solid line).

charges may exist in polyelectrolyte complexes[35] (PFN/Th-PFS) and may be attributed to their interaction with the ssDNA.

CONCLUSIONS

The electrostatic complexation of single-stranded deoxyribonucleic acid and cationic conjugated polyelectrolyte leads to significant change of fluorescence spectra of the latter, which provides a qualitative or quantitative measurement of the ssDNA molecules. PFN is suitable for detecting ssDNA at a concentration as low as 0.2 nmol/L, due to its high fluorescence quantum efficiency, molecular wire effect, as well as high affinity to ssDNA. Amplified fluorescence quenching or enhancement of PFN solution in the presence of ssDNA with different concentrations indicates that two type of structure change of the conjugated polyelectrolyte during complexation should be taken into account. Complexation-induced chain aggregation dominates at high concentration, whereas chain conformational change plays an important role at extremely low concentration of PFN. The effect of oligonucleotide sequence length on the fluorescence detection should also be examined. We also described a label-free method for ssDNA

detection based on an electrostatic complex of cationic and anionic CPEs, which exhibits resonance energy transfer between the two components. Addition of ssDNA improves the FRET extent, indicated by the obvious change of fluorescence spectra of the conjugated polyelectrolyte complex. This method of ssDNA detection is rather simple and has the advantage of tight but fast binding of cationic conjugated polyelectrolyte and ssDNA. Because the method uses spectral shape change rather than emission intensity attenuation, it is more reliable for ssDNA sensing in a biological environment with fluorescence background noise.

References

1. Shi, S.; Wudl, F. Macromolecules 1990, 23, 2119.
2. Thomas, S. W.; Joly, G. D.; Swager, T. M. Chem Rev 2007, 107, 1339.
3. Chen, L. H.; McBranch, D. W.; Wang, H. L.; Helgeson, R.; Wudl, F.; Whitten, D. G. Proc Natl Acad Sci USA 1999, 96, 12287.
4. Harrison, B. S.; Ramey, M. B.; Reynolds, J. R.; Schanze, K. S. J Am Chem Soc 2000, 122, 8561.
5. Kim, I. B.; Dunkhorst, A.; Gilbert, J.; Bunz, U. H. F. Macromolecules 2005, 38, 4560.
6. Liu, B.; Bazan, G. C. Proc Natl Acad Sci USA 2005, 102, 589.
7. Edman, L.; Pauchard, M.; Liu, B.; Bazan, G.; Moses, D.; Heeger, A. J Appl Phys Lett 2003, 82, 3961.
8. Gu, Z.; Bao, Y. J.; Zhang, Y.; Wang, M.; Shen, Q. D. Macromolecules 2006, 39, 3125.
9. Yang, R. Q.; Xu, Y. H.; Dang, X. D.; Nguyen, T. Q.; Cao, Y.; Bazan, G. C. J Am Chem Soc 2008, 130, 3282.
10. Fan, C. H.; Plaxco, K. W.; Heeger, A. J. J Am Chem Soc 2002, 124, 5642.
11. Cheng, F.; Zhang, G. W.; Lu, X. M.; Huang, Y. Q.; Chen, Y.; Zhou, Y.; Fan, Q. L.; Huang, W. Macromol Rapid Commun 2006, 27, 799.
12. Kim, I. B.; Dunkhorst, A.; Bunz, U. H. F. Langmuir 2005, 21, 7985.
13. Zhang, T.; Fan, H. L.; Zhou, J. G.; Liu, G. L.; Feng, G. D.; Jin, Q. H. Macromolecules 2006, 39, 7839.
14. Wosnick, J. H.; Mello, C. M.; Swager, T. M. J Am Chem Soc 2005, 127, 3400.
15. Wang, S.; Bazan, G. C. Adv Mater 2003, 15, 1425.
16. Lee, K.; Povlich, L. K.; Kim, J. Adv Funct Mater 2007, 17, 2580.
17. He, F.; Tang, Y. L.; Wang, S.; Li, Y. L.; Zhu, D. B. J Am Chem Soc 2005, 127, 12343.
18. Tang, Y. L.; Feng, F. D.; He, F.; Wang, S.; Li, Y. L.; Zhu, D. B. J Am Chem Soc 2006, 128, 14972.
19. Ho, H. A.; Boissinot, M.; Bergeron, M. G.; Corbeil, G.; Dore, K.; Boudreau, D.; Leclerc, M. Angew Chem Int Ed 2002, 41, 1548.
20. Gaylord, B. S.; Heeger, A. J.; Bazan, G. C. Proc Natl Acad Sci USA 2002, 99, 10954.
21. Liu, B.; Gaylord, B. S.; Wang, S.; Bazan, G. C. J Am Chem Soc 2003, 125, 6705.
22. Wang, S.; Gaylord, B. S.; Bazan, G. C. J Am Chem Soc 2004, 126, 5446.
23. Chen, L. H.; Xu, S.; McBranch, D.; Whitten, D. J Am Chem Soc 2000, 122, 9302.
24. Wu, M. Y.; Kaur, P.; Yue, H. J.; Clemmens, A. M.; Waldeck, D. H.; Xue, C. H.; Liu, H. Y. J Phys Chem B 2008, 112, 3300.
25. Abe, S.; Chen, L. H. J Polym Sci Part B: Polym Phys 2003, 41, 1676.
26. Chen, Y.; Fan, Q. L.; Wang, P.; Zhang, B.; Huang, Y. Q.; Zhang, G. W.; Lu, X. M.; Chan, H. S. O.; Huang, W. Polymer 2006, 47, 5228.
27. Huang, F.; Wu, H.; Wang, D.; Yang, W.; Cao, Y. Chem Mater 2004, 16, 708.
28. Parakka, J. P.; Jeevarajan, J. A.; Jeevarajan, A. S.; Kispert, L. D.; Cava, M. P. Adv Mater 1996, 8, 54.
29. Zhou, Q.; Swager, T. M. J Am Chem Soc 1995, 117, 12593.
30. Hong, L.; Schroth, G. P.; Matthews, H. R.; Yau, P.; Bradbury, E. M. J Biol Chem 1993, 268, 305.
31. Jezewska, M. J.; Kim, U. S.; Bujalowski, W. Biochemistry 1996, 35, 2129.
32. Spink, C. H.; Chaires, J. B. J Am Chem Soc 1997, 119, 10920.
33. Nguyen, T. Q.; Martini, I. B.; Liu, J.; Schwartz, B. J. J Phys Chem B 2000, 104, 237.
34. Ganachaud, F.; Elaissari, A.; Pichot, C.; Laayoun, A.; Cros, P. Langmuir 1997, 13, 701.
35. Vishalakshi, B.; Ghosh, S.; Kalpagam, V. Polymer 1993, 34, 3270.